










ORIGINAL RESEARCH OPEN ACCESS

Specific Calcium Signal Responses in Human Keloid-Derived Fibroblasts During Cyclical Stretching: Basic Research

Kazuhide Mineda¹  | Katsuya Sato²  | Tasuku Nakahara³  | Kazuyuki Minami³ | Kenta Ikushima¹  | Makoto Mizuguchi¹ | Shunsuke Mima¹  | Hiroyuki Yamasaki¹  | Shinji Nagasaka¹  | Yutaro Yamashita¹ | Yoshiro Abe¹  | Ichiro Hashimoto¹ 

¹Plastic and Reconstructive Surgery, School of Medicine, Tokushima University, Tokushima City, Japan | ²Graduate School of Technology, Industrial and Social Sciences, Tokushima University, Tokushima City, Japan | ³Graduate School of Sciences and Technology for Innovation, Yamaguchi University, Ube City, Japan

Correspondence: Kazuhide Mineda (k.mineda@tokushima-u.ac.jp)

Received: 17 September 2024 | **Revised:** 21 December 2024 | **Accepted:** 17 January 2025

Funding: This work was supported by JSPS KAKENHI Grant Number JP 19K10009 and 23K09081, Japan.

Keywords: calcium oscillation | calcium signal response | calcium spike | cyclical stretching | intracellular Ca^{2+} | keloid

ABSTRACT

Background: Keloids most commonly develop in the regions where the skin is constantly stretched. Although some keloid-derived fibroblasts exhibit higher single calcium spikes than normal dermal fibroblasts during short-time cyclical stretching, the calcium signal responses to long-time stretching remain unclear.

Methods: This study compared the intracellular Ca^{2+} dynamics induced by cyclical stretching stimuli between the control group (normal dermal fibroblasts) and the keloid group (keloid-derived fibroblasts). Each group was cyclically exposed to a two-dimensional stretch (10% strain). A confocal laser microscope was used to examine intracellular Ca^{2+} for 30 min fluorescently. The fluorescence intensity ratio (Fluo-8H/calcein red-orange) was used to evaluate intracellular Ca^{2+} concentration every 0.5 s. A calcium spike was a transient ratio increase of $\geq 20\%$. Receiver operating characteristic analysis was performed to determine the cutoff value of a normal calcium spike.

Results: No significant difference was observed between the keloid and control groups in the calcium signal response-positive rates (26.9% vs. 25.0%; $p = 0.9$). However, the calcium spike amplitudes were significantly higher in the keloid group than in the control group (1.66 vs. 1.41; $p = 0.02$). The cutoff value was 2.12, and 9.6% of keloid-derived fibroblasts exhibited multiple hypercalcium spikes.

Discussion: We are conducting further research based on the hypothesis that this keloid-specific subpopulation triggers the pathogenesis of keloid formation, that is, collagen overproduction, accelerated angiogenesis, and chronic inflammation.

1 | Introduction

Keloid formation commonly occurs in people with darker skin of both sexes, such as Black and Hispanic populations [1, 2]. It is often associated with hypersensitivity, pruritus, or pain [3]. Additionally, keloids tend to develop on body parts exposed to constant

stretching, such as the anterior chest, abdomen, scapular region, and upper arm [4]. There is no definitive curative treatment based on detailed molecular biological evidence [5].

Clinically, keloids grow horizontally in characteristic shapes depending on their location. For example, keloids on the

Abbreviations: ER, endoplasmic reticulum; ROC, receiver operating characteristic; TRPV4, transient receptor potential vanilloid 4.

This is an open access article under the terms of the [Creative Commons Attribution-NonCommercial-NoDerivs](https://creativecommons.org/licenses/by-nc-nd/4.0/) License, which permits use and distribution in any medium, provided the original work is properly cited, the use is non-commercial and no modifications or adaptations are made.

© 2025 The Author(s). *Health Science Reports* published by Wiley Periodicals LLC.

anterior chest grow in a crab's claw-like pattern, whereas shoulder keloids have a "butterfly" shape. These patterns reflect the predominant directions of skin tension in these regions [6]. Akaishi et al. revealed high skin tension at the keloid edges and lower tension at the keloid centers by finite-element analysis of the mechanical force distribution around keloids [7].

Most studies reporting the results of stretching stimuli to keloid-derived fibroblasts have investigated genes and protein expressions in cells before and after cyclical stretching on a stretch device by quantitative real-time polymerase chain reaction and afterward by enzyme-linked immunosorbent assay. For example, cyclic stretching for cultured keloid-derived fibroblasts is downregulated by tissue inhibitors of metalloproteinase-2, which suppress collagen production [8]. Cyclic stretching for keloid-derived microvascular endothelial cells increased endothelin-1 gene expression and secretion and involved collagen overproduction [9]. However, the definitive mechanism of keloid formation has not been elucidated.

We developed an original stretch device that enables real-time observation of intracellular Ca^{2+} dynamics during stretching because the stretching device design made it difficult to perform real-time detail observation under a microscope [10]. We have previously used this stretch device to report real-time changes in intracellular Ca^{2+} concentrations between keloid-derived fibroblasts and normal human-derived dermal fibroblasts during a 5-min cyclical stretching [11].

The results showed that approximately 10% of keloid-derived fibroblasts had a single excessive calcium spike not observed in normal skin-derived fibroblasts. The intracellular calcium concentration increases with transient receptor potential C3, a mechanosensitive calcium channel, which promotes fibronectin overexpression via the nuclear factor-kappa B pathway in fibroblasts [12]. This specific calcium spike can involve mechanisms other than fibronectin in keloid formation. However, a limitation of the previous study was the short observation time of 5 min.

In this study, the observation time was extended to 30 min, which is the limit of the real-time observation on the confocal laser microscope. This study aimed to demonstrate specific

responses of keloid skin-derived fibroblasts during cyclical stretching by evaluating these response characteristics.

2 | Materials and Methods

2.1 | Original Stretch Device and Cyclical Stretching Pattern

In this study, an originally developed cell-stretching device consisting of 134 thin transparent silicone sheets was used [13]. The sheets were placed between a fixed and a movable block made of light-curing resin in a 35-mm-diameter glass bottom dish (Figure 1a). Manipulators are attached to the microscope stage (Figure 1b) and are each fitted with a metal needle driven under computer control to stretch the silicon sheet horizontally.

In this study, cells underwent cyclical stretching (10% strain) using a stretching pattern that simulated thoracic movements associated with breathing, similar to our previous study [11].

As the pilot study, it was confirmed that fibroblasts did not peel off the silicone sheet during long-term cyclical stretching (30 min).

2.2 | Prepared Cells, Culture Procedure, and Fluorescent Labeling

The normal dermal fibroblasts (control group) and keloid-derived fibroblasts (keloid group) were cultured by the explant method from three different patients' samples (Table 1). The remaining dermis was dissected into small blocks, arranged on 10-cm dish, and incubated under explant conditions (37°C, 5% CO_2) with fibroblast growth medium (PromoCell, Germany). The medium was replaced every 2–3 days, and cells were used in experiments during passages 2 or 3.

Our previous study reported that the silicone sheets were coated with fibronectin to enhance cellular adhesion [10]. Normal and keloid-derived fibroblasts were then seeded onto the device at a density of 100,000 cells/dish and incubated overnight. After preincubation, Fluo-8H (AAT Bioquest Inc., USA) and calcein

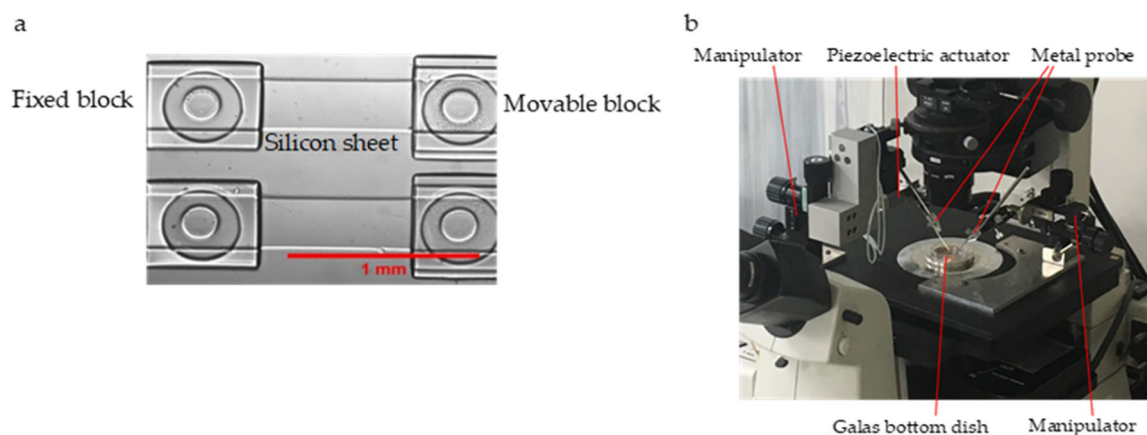


FIGURE 1 | Structure and operating environment of the stretch device. (a) The cell-stretching microchamber consists of a 5- μm -thick transparent silicone elastomer and extension structures, including a movable and a fixed block. (b) Manipulators are attached to the microscope stage. These manipulators are each fitted with a metal needle driven under computer control.

red–orange (Thermo Fisher Scientific, USA) were, respectively, used as markers of intracellular Ca^{2+} and cytoplasm.

This protocol was approved by the ethics review committee of Tokushima University Hospital (approval number: 2835-1).

2.3 | Fluorescent Observation and Image Analysis

Cells adhering to the sheets were checked under a microscope, and sheets with dense or sparse cells were excluded. Since one experimental system is limited to observing one sheet, the experiment was repeated at least 10 times in each group.

A confocal laser microscope, Nikon A1R, was used for fluorescence observation to capture the intracellular Ca^{2+} and cytoplasm every 0.5 s (Figure 2 and Video S1). The fluorescence intensity ratio was defined as the fluorescence intensities of Fluo-8H/calcein red–orange. By calculating the ratio used by ImageJ software (NIH), intracellular Ca^{2+} changes were normalized and quantitatively evaluated.

2.4 | Definition of Positive Calcium Signal Response

A positive calcium signal response (calcium spike) was defined as a spike that could be clearly determined as a transient increase in fluorescence intensity ratio by $\geq 20\%$. Furthermore,

TABLE 1 | Profiles of cultured fibroblasts derived from control and keloid groups.

	Number	Sex	Age (years)	Location
Control	1	F	8	Back
	2	F	48	Abdomen
	3	F	2	Abdomen
Keloid	1	M	32	Precordium
	2	F	20	Precordium
	3	F	38	Abdomen

Note: F: Female, M: Male.

assuming that all control fibroblasts had normal responsive peaks of the intracellular Ca^{2+} concentration, receiver operating characteristic (ROC) analysis was performed to determine the cutoff value.

2.5 | Statistics

Two researchers analyzed the results of 5–10 observable cells per silicone sheet without blinding. All results are expressed as medians [interquartile ranges] for each condition. SPSS Statistics v25 (IBM, USA) was used to evaluate the statistical differences between the groups. Fisher's exact test, Mann–Whitney U test, and ROC analysis were conducted, and a p -value < 0.05 was considered significant.

3 | Results

3.1 | Calcium Signal Response-Positive Rates Between the Control and Keloid Groups

Figure 3 showed real-time dynamics of the intracellular Ca^{2+} in individual cells, based on the fluorescence intensity ratio. The calcium signal response-positive rates in the control group were 25.0% (6/24 cells), 16.0% (4/25 cells), and 28.1% (9/32 cells) (Figure 3a, left), whereas the rates in the keloid groups were 26.9% (7/26 cells), 19.2% (5/26 cells), and 29.0% (9/31 cells) (Figure 3a, right). No significant difference was observed in the median rates of the keloid (26.9% [23.0% to 30.0%]) and control (25.0% [20.5% to 26.6%]) (Figure 3b; $p = 0.9$).

3.2 | Higher Calcium Spikes in the Keloid Than in the Control Groups

When only calcium signal response-positive cells were collected in each group, the keloid group had many cells with higher calcium spikes than the control group (Figure 4a).

The median peak value was 1.66 [1.45 to 2.25] in the keloid group, which was significantly higher than 1.41 [1.27–1.63] in the control group (Figure 4b; $p = 0.02$). The maximum peak

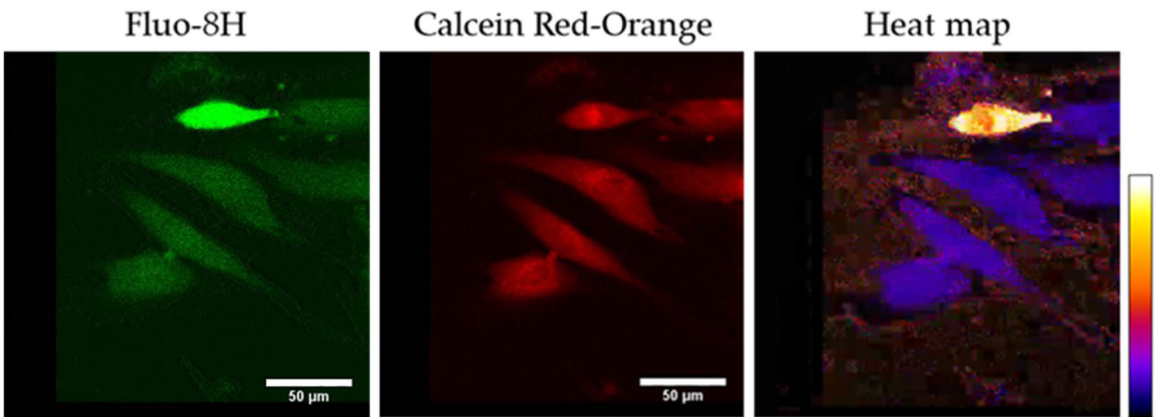


FIGURE 2 | Fluorescence images and visual heatmaps. Intracellular Ca^{2+} and cytoplasm were intermittently captured. The fluorescence intensity ratios were used to create heat maps illustrating intracellular Ca^{2+} dynamics.

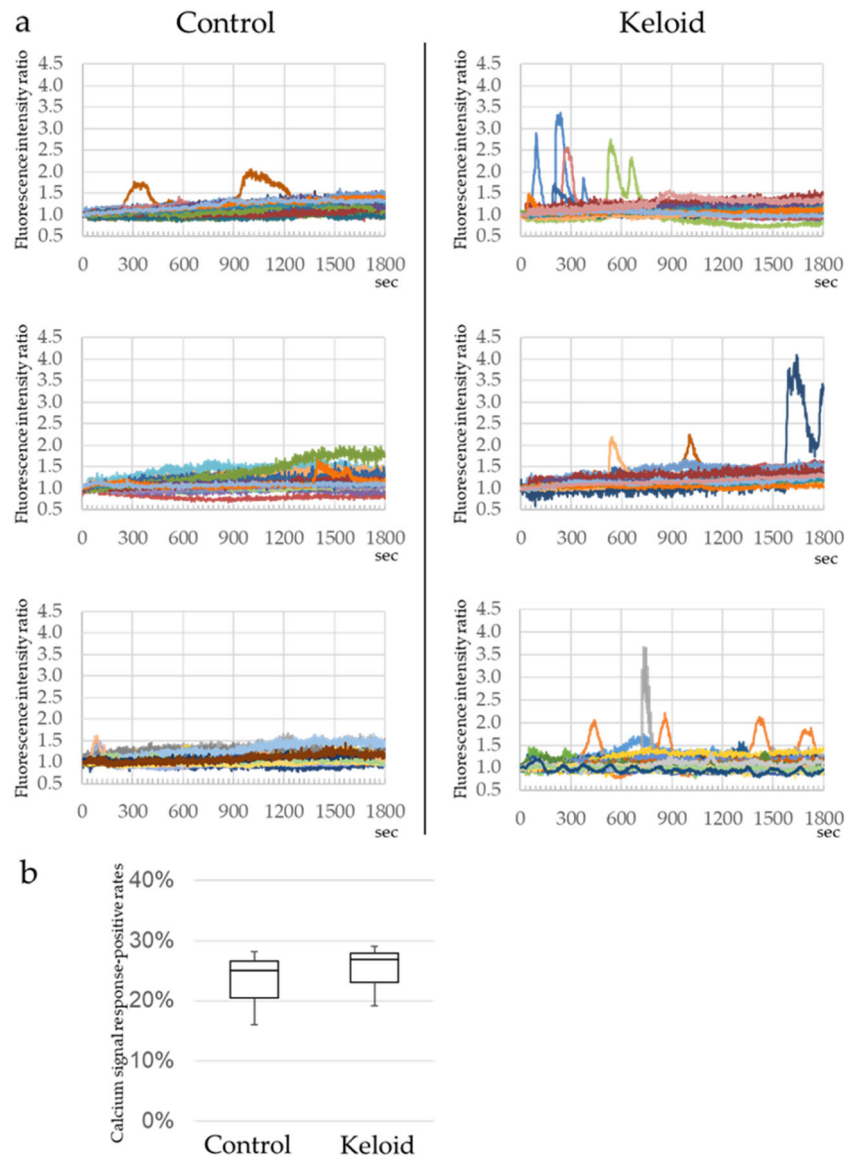


FIGURE 3 | Real-time dynamics of the intracellular Ca^{2+} in the control and keloid groups. (a) In the control group, calcium signal response-positive rates were 25.0%, 16.0%, and 28.1%, respectively. The rates were 26.9%, 19.2%, and 29.0%, respectively, in the keloid group. (b) The median response-positive rates were not significant between the keloid and control groups ($p = 0.9$).

value of each cell in the control and keloid groups was analyzed for the ROC curve, and the cutoff value within the normal range was 2.12 (Figure 4c). About 9.6% of keloid-derived fibroblasts had an excessive influx of intracellular Ca^{2+} above the normal range during cyclical stretching.

3.3 | More Calcium Oscillations in the Keloid Than in the Control Groups

Only in calcium signal response-positive cells, compared to the average of approximately 70% that showed only single calcium spike in control groups, more than the average half of keloid groups showed multiple calcium spikes (calcium oscillations), and approximately 5% of them showed as many as 9 calcium spikes (Figure 5). Furthermore, keloid-derived fibroblasts showed a tendency for higher calcium spikes to produce more oscillations.

4 | Discussion

Calcium ion (Ca^{2+}) is a second messenger, fulfilling a plethora of intracellular functions, such as neurotransmitter release, muscle contraction, secretion, synaptic plasticity, and apoptosis [13–15]. Under normal conditions, the intracellular Ca^{2+} concentration is kept very low, and an increase in the concentration triggers downstream signaling cascades [16].

Advances in the definition of calcium signal responses provided evidence of the high spatiotemporal complexity and asynchronicity of intracellular Ca^{2+} [17, 18]. These responses are represented by localized calcium spikes that gradually propagate into the cell as calcium waves [19, 20]. In our previous 5-min observation [10], the calcium signal response rates were significantly higher in the keloid group than in the control group (4.5% vs. 15.7%). However, this study found that the calcium spikes were asynchronously induced after 5 min during cyclical

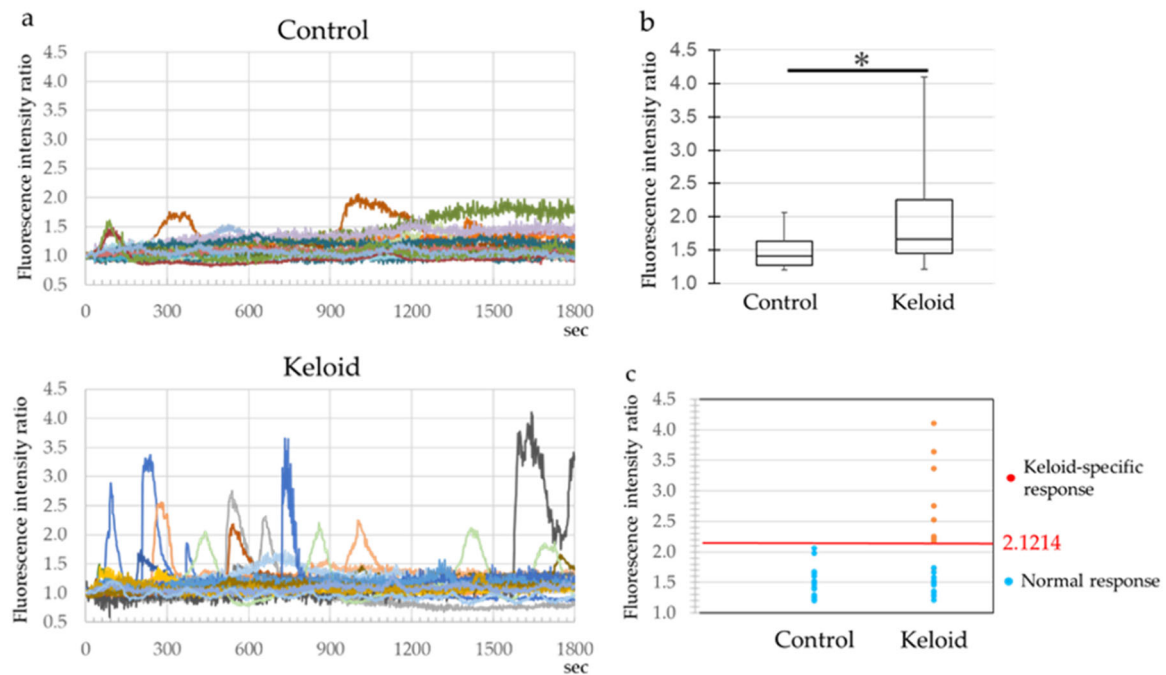


FIGURE 4 | Differences in peak calcium spike values between the control and keloid groups. (a) In both groups, only calcium signal response-positive fibroblasts were collected. (b) The median peak value of calcium spikes was 1.66 in the keloid group, significantly higher than 1.41 in the control group ($p = 0.02$). (c) The maximum peak value of each cell in the control and keloid groups was analyzed for the receiver operating characteristic curve, and the cutoff value within the normal range was 2.12.

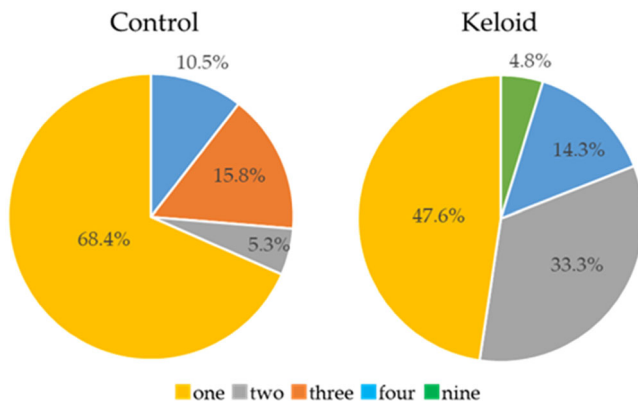


FIGURE 5 | Differences in calcium oscillation between the control and keloid groups. Only in calcium signal response-positive cells, more than the average half of keloid groups showed multiple calcium spikes, and approximately 5% of these showed as many as nine spikes.

stretching and were not significantly different between the two groups. Furthermore, calcium oscillations with multiple calcium spikes were observed for the first time in both groups.

The correlation between calcium spikes and various physiological responses remains poorly understood. The downstream calcium signal responses (secretion, gene expression, proliferation, and so on) are controlled by oscillations and detailed characteristics such as amplitude, baseline, and sustainability [21]. In this study, the baseline Ca^{2+} levels were almost constant between the control and keloid groups, including nonresponsive cells (no calcium spikes). However, the frequency and amplitude of calcium spikes were disjointed in the response-positive cells. Approximately 10% of keloid-derived fibroblasts had excessive calcium spikes above

normal based on ROC analysis, comparable to our previous study and inferred to be a keloid-specific subpopulation. New evidence is that this subpopulation showed multiple oscillations above four, including nine times in 30 min. We hypothesize that this minor subpopulation triggers the pathogenesis of keloid formation, that is, collagen overproduction, accelerated angiogenesis, and chronic inflammation. However, because this study was conducted using monolayer cultures in vitro, reproducing the calcium signal response to stretching was limited for keloids in vivo.

An abnormal increase of intracellular Ca^{2+} has been observed in the neutrophils in human cystic fibrosis compared with those in noncystic fibrosis. Transient receptor potential vanilloid 4 (TRPV4) is responsible for the excessive Ca^{2+} influx into the neutrophil cells [22]. TRPV2 is responsible for a sustained increase of the intracellular Ca^{2+} in myogenic cells of animal models with dilated cardiomyopathy [23]. A recent study has shown that tranilast, as a TRPV2 antagonist, suppresses the abnormal increase of intracellular Ca^{2+} and improves cardiomyopathy with heart failure in vivo [24].

Tranilast has a prophylactic effect on keloid development but is not sufficiently effective to ameliorate keloids [25]. Verapamil, a calcium antagonist, has also been reported to relieve pain and itching and inhibit erythema and hypertrophy in keloids, but to a limited extent [26–29]. Lee reported that cyclical stretching induced calcium spike through a mechanosensitive channel in human dermal fibroblasts and that the calcium spike was suppressed by a Ca^{2+} channel blocker [30]. Sakamoto et al. reported that decreased mitochondrial complex activities and abnormal mitochondria were detected in keloid-derived fibroblasts under normoxic conditions and that glycolysis is enhanced and mitochondrial function is impaired under hypoxia

[31]. Wang et al. reported that electron microscope examinations revealed increased dysmorphic mitochondria and expanded endoplasmic reticulum (ER) in human keloid tissue. They noted the contributions of mitochondrial dysfunction and dysregulated ER stress signaling in human keloid formation [32]. Since the ER and mitochondria are stores of intracellular Ca^{2+} , it is possible that their organic or functional abnormalities are related to Ca^{2+} dynamics as a second messenger. Based on the above, we speculated that multiple excessive calcium spikes in keloid-specific subpopulations were caused by dysregulation of mechanosensitive Ca^{2+} channels as TRPV2, ER, and mitochondria in keloid-derived fibroblasts (Figure S1). We are attempting to isolate and culture this subpopulation using single-cell culture methods.

Therefore, if this keloid-specific subpopulation can be isolated, it will be possible to study the relationship between stretch stimuli and intracellular Ca^{2+} and functional and organic abnormalities in mitochondria and ER. Ultimately, the focus should be on whether normalization of the keloid-specific calcium signaling response can inhibit the physiological characteristics of keloid formation. Thus, we will try to identify the causes of this dysregulation and develop agents capable of normalizing the keloid-specific calcium signal response.

Author Contributions

Kazuhide Mineda: conceptualization, formal analysis, funding acquisition, investigation, methodology, project administration, validation, writing – original draft, writing – review and editing. **Katsuya Sato:** formal analysis, investigation, visualization. **Tasuku Nakahara:** methodology. **Kazuyuki Minami:** methodology. **Kenta Ikushima:** data curation. **Makoto Mizuguchi:** data curation. **Shunsuke Mima:** data curation. **Hiroyuki Yamasaki:** data curation. **Shinji Nagasaka:** data curation. **Yutaro Yamashita:** formal analysis. **Yoshiro Abe:** formal analysis. **Ichiro Hashimoto:** supervision.

Acknowledgments

This study was technically supported by the Support Center for Advanced Medical Sciences Institute of Health Biosciences, Tokushima University Graduate School. The authors thank Enago (www.enago.jp) for the English language review. This work was supported by JSPS KAKENHI Grant Number JP 19K10009 and 23K09081, Japan. All authors have read and approved the final version of the manuscript [CORRESPONDING AUTHOR or MANUSCRIPT GUARANTOR] had full access to all of the data in this study and takes complete responsibility for the integrity of the data and the accuracy of the data analysis.

Ethics Statement

The study was conducted in accordance with the Declaration of Helsinki. The study was approved by the ethics review committee of Tokushima University Hospital (protocol code: 2835-1 and date of approval: March 15, 2017). Informed consent was obtained from all subjects involved in the study.

Conflicts of Interest

The authors declare no conflicts of interest.

Data Availability Statement

Our cell-stretching device is patented (Patent No. 4931017). Information is available on request to researchers interested in this device.

Experimental data can also be disclosed. Please contact the corresponding author (e-mail: k.mineda@tokushima-u.ac.jp).

Transparency Statement

The lead author Kazuhide Mineda affirms that this manuscript is an honest, accurate, and transparent account of the study being reported; that no important aspects of the study have been omitted; and that any discrepancies from the study as planned (and, if relevant, registered) have been explained.

References

1. F. B. Niessen, P. H. M. Spauwen, J. Schalkwijk, and M. Kon, "On the Nature of Hypertrophic Scars and Keloids: A Review," *Plastic and Reconstructive Surgery* 104 (1999): 1435–1458.
2. S. K. Kiprono, B. M. Chaula, J. E. Masenga, J. W. Muchunu, D. R. Mavura, and M. Moehrle, "Epidemiology of Keloids in Normally Pigmented Africans and African People With Albinism: Population-Based Cross-Sectional Survey," *British Journal of Dermatology* 173 (2015): 852–854.
3. T. L. Tuan and L. S. Nichter, "The Molecular Basis of Keloid and Hypertrophic Scar Formation," *Molecular Medicine Today* 4 (1998): 19–24.
4. R. Ogawa, K. Okai, F. Tokumura, et al., "The Relationship Between Skin Stretching/Contraction and Pathologic Scarring: The Important Role of Mechanical Forces in Keloid Generation," *Wound Repair and Regeneration* 20 (2012): 149–157.
5. A. Al-Attar, S. Mess, J. M. Thomassen, C. L. Kauffman, and S. P. Davison, "Keloid Pathogenesis and Treatment," *Plastic and Reconstructive Surgery* 117 (2006): 286–300.
6. R. Ogawa, "Mechanobiology of Scarring," *Wound Repair and Regeneration* 19 (2011): S2–S9.
7. S. Akaishi, M. Akimoto, R. Ogawa, and H. Hyakusoku, "The Relationship Between Keloid Growth Pattern and Stretching Tension: Visual Analysis Using the Finite Element Method," *Annals of Plastic Surgery* 60 (2008): 445–451.
8. T. Dohi, K. Miyake, M. Aoki, et al., "Tissue Inhibitor of Metalloproteinase-2 Suppresses Collagen Synthesis in Cultured Keloid Fibroblasts," *Plastic and Reconstructive Surgery - Global Open* 3 (2015): e520.
9. K. Kiya, T. Kubo, K. Kawai, et al., "Endothelial Cell-Derived Endothelin-1 Is Involved in Abnormal Scar Formation by Dermal Fibroblasts Through RhoA/Rho-Kinase Pathway," *Experimental Dermatology* 26 (2017): 705–712.
10. K. Sato, Y. Ogawa, S. Ito, S. Fujisawa, and K. Minami, "Strain Magnitude Dependent Intracellular Calcium Signaling Response to Uniaxial Stretch in Osteoblastic Cells," *Journal of Biomechanical Science and Engineering* 10 (2015): 15-00242, <https://doi.org/10.1299/jbse.15-00242>.
11. K. Mineda, K. Sato, T. Nakahara, et al., "Cyclical Stretching Induces Excess Intracellular Ca^{2+} Influx in Human Keloid-Derived Fibroblasts *In Vitro*," *Plastic & Reconstructive Surgery* 151 (2023): 346–354.
12. H. Ishise, B. Larson, Y. Hirata, et al., "Hypertrophic Scar Contraction Is Mediated by the TRPC3 Mechanical Force Transducer via Nfkb Activation," *Scientific Reports* 5 (2015): 11620.
13. K. Minami, T. Hayashi, K. Sato, and T. Nakahara, "Development of Micro Mechanical Device Having Two-Dimensional Array of Micro Chambers for Cell Stretching," *Biomedical Microdevices* 20 (2018): 10.
14. E. Carafoli and J. Krebs, "Why Calcium? How Calcium Became the Best Communicator," *Journal of Biological Chemistry* 291 (2016): 20849–20857.
15. S. Patergnani, A. Danese, E. Bouhamida, et al., "Various Aspects of Calcium Signaling in the Regulation of Apoptosis, Autophagy, Cell Proliferation, and Cancer," *International Journal of Molecular Sciences* 21 (2020): 8323.

16. C. Giorgi, A. Danese, S. Missiroli, S. Patergnani, and P. Pinton, "Calcium Dynamics as a Machine for Decoding Signals," *Trends in Cell Biology* 28 (2018): 258–273.
17. M. D. Bootman and G. Bultynck, "Fundamentals of Cellular Calcium Signaling: A Primer," *Cold Spring Harbor Perspectives in Biology* 12 (2020): a038802.
18. J. García-Sancho and A. Verkhratsky, "Cytoplasmic Organelles Determine Complexity and Specificity of Calcium Signalling in Adrenal Chromaffin Cells," *Acta Physiologica* 192 (2008): 263–271.
19. M. J. Berridge, "The Versatility and Complexity of Calcium Signaling," *Novartis Foundation Symposium* 239 (2001): 52–64.
20. H. Cheng and W. J. Lederer, "Calcium Sparks," *Physiological Reviews* 88 (2008): 1491–1545.
21. G. Dupont, L. Combettes, G. S. Bird, and J. W. Putney, "Calcium Oscillations," *Cold Spring Harbor Perspectives in Biology* 3 (2011): a004226.
22. G. Dupont and L. Combettes, "Fine Tuning of Cytosolic Ca^{2+} Oscillations," *FI000Research* 5 (2016): 2036.
23. A. Rimessi, V. A. M. Vitto, S. Patergnani, and P. Pinton, "Update on Calcium Signaling in Cystic Fibrosis Lung Disease," *Frontiers in Pharmacology* 12 (2021): 581645.
24. Y. Iwata, S. Ito, S. Wakabayashi, and M. Kitakaze, "TRPV2 Channel as a Possible Drug Target for the Treatment of Heart Failure," *Laboratory Investigation* 100 (2020): 207–217.
25. T. Matsumura, M. Matsui, Y. Iwata, et al., "A Pilot Study of Tranilast for Cardiomyopathy of Muscular Dystrophy," *Internal Medicine* 57 (2018): 311–318.
26. F. Margaret Shanthi, K. Ernest, and P. Dhanraj, "Comparison of Intralesional Verapamil With Intralesional Triamcinolone in the Treatment of Hypertrophic Scars and Keloids," *Indian Journal of Dermatology, Venereology and Leprology* 74 (2008): 343–348.
27. R. B. Ahuja and P. Chatterjee, "Comparative Efficacy of Intralesional Verapamil Hydrochloride and Triamcinolone Acetonide in Hypertrophic Scars and Keloids," *Burns* 40 (2014): 583–588.
28. R. Abedini, P. Sasani, H. R. Mahmoudi, M. Nasimi, A. Teymourpour, and Z. Shadlou, "Comparison of Intralesional Verapamil Versus Intralesional Corticosteroids in Treatment of Keloids and Hypertrophic Scars: A Randomized Controlled Trial," *Burns* 44 (2018): 1482–1488.
29. N. Saki, R. Mokhtari, and F. Nozari, "Comparing the Efficacy of Intralesional Triamcinolone Acetonide With Verapamil in Treatment of Keloids: a Randomized Controlled Trial," *Dermatology Practical & Conceptual* 9 (2019): 4–9.
30. R. C. Lee, "The Response of Burn Scars to Intralesional Verapamil: Report of Five Cases," *Archives of Surgery* 129 (1994): 107–111.
31. Y. Sakamoto, M. Ishijima, H. Kaneko, et al., "Distinct Mechanosensitive Ca^{2+} Influx Mechanisms in Human Primary Synovial Fibroblasts," *Journal of Orthopaedic Research* 28 (2010): 859–864.
32. Q. Wang, P. Wang, Z. Qin, et al., "Altered Glucose Metabolism and Cell Function in Keloid Fibroblasts Under Hypoxia," *Redox Biology* 38 (2021): 101815.

Supporting Information

Additional supporting information can be found online in the Supporting Information section.